

Assessing the thermal conductivity of non-uniform thin-films: Nanocrystalline Cu composites incorporating carbon nanotubes

Stephen D. Kang, Jung Joon Yoo, Ho-Ki Lyeo, Jae Yong Song, Sungjun Lee et al.

Citation: *J. Appl. Phys.* **110**, 023506 (2011); doi: 10.1063/1.3606559

View online: <http://dx.doi.org/10.1063/1.3606559>

View Table of Contents: <http://jap.aip.org/resource/1/JAPIAU/v110/i2>

Published by the [American Institute of Physics](#).

Related Articles

Thermal transport in grain boundary of graphene by non-equilibrium Green's function approach
Appl. Phys. Lett. **101**, 043112 (2012)

Determination of the thermal conductivity tensor of the n=7 Aurivillius phase Sr₄Bi₄Ti₇O₂₄
Appl. Phys. Lett. **101**, 021904 (2012)

Edge effect on thermal transport in graphene nanoribbons: A phonon localization mechanism beyond edge roughness scattering
Appl. Phys. Lett. **101**, 013101 (2012)

Thermal conductivity modeling of periodic porous silicon with aligned cylindrical pores
J. Appl. Phys. **111**, 124329 (2012)

Phonon interference and its effect on thermal conductance in ring-type structures
J. Appl. Phys. **111**, 113531 (2012)

Additional information on J. Appl. Phys.

Journal Homepage: <http://jap.aip.org/>

Journal Information: http://jap.aip.org/about/about_the_journal

Top downloads: http://jap.aip.org/features/most_downloaded

Information for Authors: <http://jap.aip.org/authors>

ADVERTISEMENT



IBD Optical Film Quality at PVD Rates

Advanced Optical Thin Films

Wide Range of Applications

Superior Throughput and Repeatability

SPECTOR-HT ION BEAM DEPOSITION SYSTEMS

Veeco
Innovation. Performance. Brilliant.

www.veeco.com/spectorht

Assessing the thermal conductivity of non-uniform thin-films: Nanocrystalline Cu composites incorporating carbon nanotubes

Stephen D. Kang,^{1,a)} Jung Joon Yoo,² Ho-Ki Lyoo,^{1,b)} Jae Yong Song,¹ Sungjun Lee,¹ and Jin Yu²

¹Korea Research Institute of Standards and Science, Daejeon, 305-340, Republic of Korea

²Department of Materials Science and Engineering, Korea Advanced Institute of Science and Technology, Daejeon 305-701, Republic of Korea

(Received 18 May 2011; accepted 28 May 2011; published online 20 July 2011)

We demonstrate a procedure for measuring the thermal conductivity of non-ideal thin-films with significant non-uniformity. By spatially mapping the thermal transport with time-domain thermoreflectance measurements, followed by statistical analysis, we determined the thermal conductivity of Cu composite films containing dispersed carbon nanotubes (CNTs). The thermal conductivity of the composite decreased from 188 to 60 W/m K as 1.8 wt. % of multi-walled CNTs was incorporated into nanocrystalline Cu. We compared the decreasing trend with that calculated from a scattering model to find out that the CNTs scatter the heat carriers in Cu. © 2011 American Institute of Physics. [doi:10.1063/1.3606559]

I. INTRODUCTION

Quantitative thermal conductivity measurements of thin films are conventionally applied to materials with planar uniformity. The preference for uniform materials is because most thin film measurements lack an average-out mechanism that is naturally present in bulk measurements. In addition, further difficulties are caused for thin film measurements, especially for contact methods, if any surface irregularities in the non-uniform thin film introduce ambiguity in the contact properties. Unfortunately, many interesting thin-film materials in practice exhibit planar non-uniformity. For example, composite thin-films usually have microscopic inhomogeneity which is intentionally introduced to improve the material properties. Here, through a case study, we demonstrate a simple method that allows us to determine the representative thermal conductivity of non-uniform thin-films. For this purpose, we used the time-domain thermoreflectance (TDTR) method^{1,2} with a microscopic mapping technique³ to determine thermal conductivities through statistical distributions.

As the subject material of our case study, nanocrystalline Cu composites incorporating various amounts of carbon nanotubes (CNTs) were investigated. This material system serves as a good example for our study since even a small non-uniformity in the sample can sensitively induce appreciable non-uniformities in thermal transport because of the highly contrasted physical properties of the constituents. Additionally, it is an issue of great interest to mix CNTs into a host material to enhance the thermal properties of composites. By exploiting the high thermal conductivity of CNTs, which have reported values reaching >3000 W/m K at room temperature,^{4,5} previous reports mostly showed that CNTs could enhance the thermal conductivity of insulating host-materials such as polymers⁶⁻⁹ and silica.¹⁰ On the other

hand, whether CNTs can also enhance the thermal conductivity of highly conducting metals, such as Al (237 W/m K) or Cu (401 W/m K),¹¹ remains an interesting, yet marginally studied issue.

Previously, as one attempt, Chu *et al.* measured the thermal conductivity of spark plasma sintered Cu-CNT bulk composites; large additions of multi-walled CNTs (15 vol. %) rather degraded the thermal conductivity of the bulk composite by 26.6%.¹² On the other hand, Cho *et al.* showed an increase in thermal conductivity by 3% in their spark plasma sintered Cu-CNT bulk composites containing small amounts of multi-walled CNTs (1.0 vol. %).¹³ Large additions of multi-walled CNTs (>5 vol. %) still degraded the thermal conductivity of their composites; the authors related this trend to the bundling of CNTs. The dispersion of CNTs, which is limited by the grain size of Cu since CNTs populate at the grain boundaries in Cu-CNT composites, has been considered a controlling factor for the transport property in these composites.

II. SAMPLE PREPARATION

We prepared nanocrystalline Cu-CNT thin-film composites by incorporating dispersed multi-walled CNTs (MWCNTs) into Cu *in situ* during the electrodeposition process of Cu. In this process, the repulsive force between CNTs, which makes it a dispersion solution, is present during the whole deposition period. For electrodeposition, the sample substrate served as a cathode which was prepared by sputter-depositing Cu(30 nm) and Ti(10 nm) onto Si(100) wafers. Cu plates were used for the anode. MWCNTs grown by chemical vapor deposition were purified by a HCl acid treatment process and subsequent annealing in a He atmosphere. The average diameter and wall thickness of the MWCNTs confirmed by transmission electron microscopy was 25–30 nm and ~ 8 nm, respectively. The length of the MWCNTs varied from hundreds of nanometers to ~ 1 μm . These MWCNTs were functionalized with sodium dodecyl

^{a)}Also known as Dongmin Kang.

^{b)}Author to whom correspondence should be addressed. Electronic mail: hklyeo@kriss.re.kr.

sulfate and polyacrylic acid to promote the dispersion of MWCNTs and adsorption of MWCNTs to Cu, respectively. The electrolyte was composed of copper sulfate (29 g/l), ammonium sulfate (50 g/l), and varying amounts of functionalized MWCNTs (0–15 g/l) to control the MWCNT content in the product film. Citric acid (5 g/l) was added to the electrolyte to suppress the growth of Cu grains. Electrodeposition was driven by 10 V voltage pulses of 0.2 ms width and 50 Hz frequency. After deposition, the composite films were annealed in vacuum at 200 °C for 2 h in order to remove the residual organic additives.

An Al transducer layer was sputter-deposited on top of the composite film for thermal transport measurements. Figures 1(a)–1(d) show the microstructure of the nanocomposite films observed with a field emission scanning electron microscope before depositing the top Al layer. The incorporated MWCNTs appear well-dispersed in the Cu matrix. (Hereafter we simply refer to the incorporated MWCNTs as CNTs.) The grain size of Cu is critically related to this dispersion since inhibiting the grain growth of Cu during the electrodeposition process promotes the dispersion of CNTs. In our samples, the average grain size measured with SEM was ~ 20 nm. The CNT content of the samples estimated with a carbon analyzer (Eltra CS-800) was 0, 0.5, 1.0, and 1.8 wt. % [Figs. 1(a)–1(d)]. The thickness of the Al and Cu-CNT composite layers was 56/270, 60/211, 62/207, and 83/217 nm, respectively; the thickness was measured by picosecond acoustics with complementary analysis using Rutherford backscattering spectroscopy.

III. MEASUREMENT PROCEDURE

The thermal conductivity of the samples was measured by the TDTR method,^{1,2} which probes the time-resolved change in reflectivity induced by heating the top transducer layer with a modulated pump beam. The probe beam, which probes the change in reflectivity, arrives at the sample surface with a controlled pump-to-probe delay time, and the

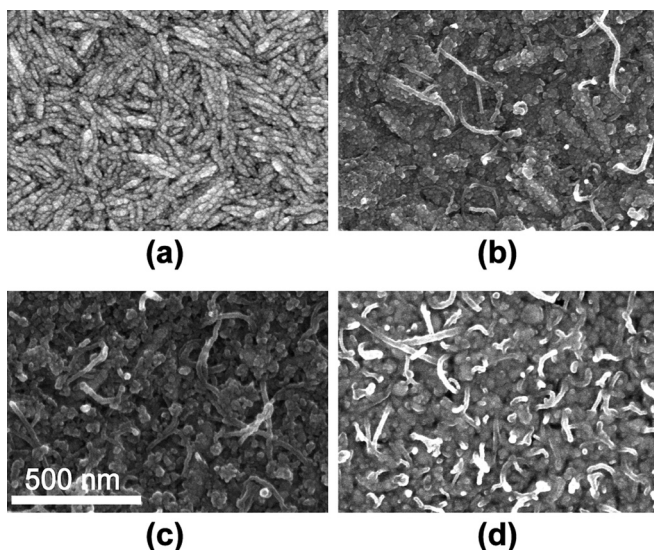


FIG. 1. SEM images of the Cu-CNT composites taken after vacuum annealing. CNT content in the samples are (a) 0 wt. %; (b) 0.5 wt. %; (c) 1.0 wt. %; (d) 1.8 wt. %.

reflected intensity is recorded as a function of delay time. The change in the reflected intensity is proportional to the rise in surface temperature, which allows us to obtain a cooling curve. In the procedure, the intensity signal of the reflected probe beam is separated into an in-phase signal (V_{in}) and out-of-phase signal (V_{out}) by an RF lock-in amplifier. We utilize the ratio $-V_{in}/V_{out}$ to analyze the thermal transport properties of the sample. The cooling curve ($-V_{in}/V_{out}$ versus time) represents the thermal transport property of a microscopic area with the size of the beam spot, which is $\sim 5.8 \mu\text{m}$ in $1/e^2$ radius in our setup.

In samples with significant non-uniformity, however, measuring the transport at a few locations does not suffice to determine the thermal conductivity of the film. Particularly, our Cu-CNT composite films exhibit variation in the cooling curves as the measurement location is shifted. These variations are mainly due to the micron-scale variation in CNT density, which affects both the thermal conductivity of the composite film and the interfacial thermal conductance between the composite film and the Al transducer layer. Furthermore, some locations on the film surface, where the CNTs protrude from the Al transducer layer, produce non-true signals coherent with the modulation frequency.

We work around these complications by mapping the in-phase to out-of-phase ratio $-V_{in}/V_{out}$ of the reflected intensity at a fixed pump-to-probe delay time,³ thereby obtaining spatial maps convertible to a distribution profile to determine the representative measurement value. During the mapping, the optical setup is fixed and only the sample is displaced by a two-dimensional (2D) motion controller. This way, 2D maps that roughly scale to the thermal effusivity $\sqrt{\Lambda C}$ (Λ = thermal conductivity, C = volumetric heat capacity) of the film are obtainable without temporal challenges. Comparing the distribution profile and the qualitative features on the $-V_{in}/V_{out}$ ratio map helps to gain insight on the distribution. Afterwards, we take full time scans of $-V_{in}/V_{out}$ over a ~ 4 ns delay time at representative locations to determine the appropriate parameters for model analysis, from which the thermal conductivity of the composite film is extracted.

IV. RESULTS AND DISCUSSION

Figures 2(a) and 2(b) show examples of the $-V_{in}/V_{out}$ ratio map obtained from the composite. The spatial resolution of these maps is roughly in the range of 2–5 μm depending on the local transport property of the sample, which is smaller than the $1/e^2$ radius of the beam size but larger than the diffraction limit.³ Higher values in the $-V_{in}/V_{out}$ ratio roughly represent higher thermal conductivities. The map obtained from a nanocrystalline Cu film without any CNT content, shown in Fig. 2(a), displays a relatively uniform thermal transport property. Figure 2(b) is a map obtained from the composite with a 0.5 wt. % CNT content. The non-uniformity in thermal transport is explicitly noticeable by the color distribution. However, we find that the abnormally high ratio values (higher than 8–9) depicted as red are false values; topologically irregular locations identified with atomic force microscopy tended to show a strong correlation

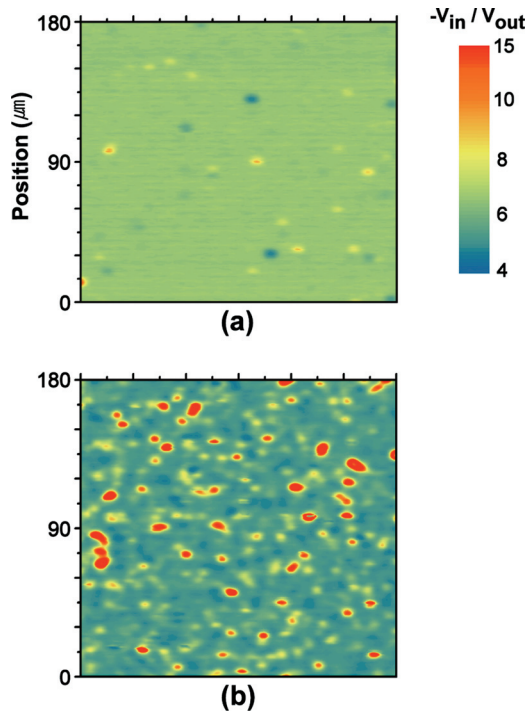


FIG. 2. (Color) Spatial maps of the $-V_{in}/V_{out}$ ratio obtained from the Cu-CNT composite with a (a) 0 wt. % and (b) 0.5 wt. % CNT content. The delay time between the pump and probe beams was fixed at 940 ps to avoid acoustic echoes. The wavelength of the beam was 785 nm and the repetition rate of the mode-locked Ti:sapphire laser was 75.8 MHz. The modulation frequency of the pump and probe beam was 9.47 MHz and 250 Hz, respectively. The powers of both beams were adjusted to ~ 8 mW.

with such spots yielding abnormally high ratio values (data not shown). These values are to be excluded from the assessment of the thermal conductivity of the sample.

For each sample, maps were obtained as shown in Fig. 2, from which the distributions of the $-V_{in}/V_{out}$ ratio were extracted and plotted in Figs. 3(a)–3(d). In the sample without CNT content, Fig. 3(a), the distribution appeared narrow and symmetric. By contrast, samples containing CNT content, Figs. 3(b)–3(d), appeared broader and asymmetric, reflecting the non-uniformity of the sample. The distribution in the film with a 1.0 wt. % CNT content, Fig. 3(c), is broader than that in the film with a 0.5 wt. % CNT content, Fig. 3(b), implying that the broad distribution is due to the variation in CNT density. Asymmetric upper tails with high

ratio values are noticeable in Figs. 3(b) and 3(c), which are due to surface irregularities as discussed previously. Note that such an upper tail is not present in the distribution in Fig. 3(d). Compared to other samples, the Al transducer layer is > 20 nm thicker in this sample, making it less vulnerable to surface irregularities. This fact supports our interpretation of the abnormally high ratios observed in other samples.

From the distributions in Figs. 3(a)–3(d), we assign the most frequent value in each distribution as the representative value of the composite film. This way, non-true high ratio values are naturally excluded. In addition, the most frequent value resembles the value corresponding to the average thermal transport, provided that the distribution in thermal transport properties is closely symmetric near the peak value. By paying attention to the most frequent value, a consecutive down-shift is noticeable as the CNT content increases in the composite film. This decreasing trend indicates that the thermal conductivity of the sample has degraded with the addition of CNTs.

To quantitatively investigate the trend in thermal conductivity Λ , Λ was extracted by model-analyzing the cooling curves obtained at locations that yield the previously determined representative values. Any thickness variations are taken into account in this model-analysis. Details of the analysis procedure are described in Ref. 2. Figure 4 shows the result of the procedure for the sample with a 0.5 wt. % CNT content. The determined Λ values of all of the samples are plotted in Fig. 5.

The value of Λ obtained from nanocrystalline Cu without any CNT content was $\Lambda \approx 188$ W/m K (Fig. 5), which is 47% of the accepted bulk value 401 W/m K of Cu,¹¹ and 69% of the reported value 272 W/m K of an evaporated Cu thin film with 181 nm thickness.¹⁴ Considering that the heat conduction in Cu is dominated by the electronic contribution, the nanogranular microstructure [Fig. 1(a)] with grain sizes (~ 20 nm) significantly smaller than the electronic mean free path of Cu (39 nm) primarily accounts for the low value of our nanocrystalline Cu films.¹⁵ For reference, the thermal conductivity of sputter deposited Cu films with larger grain sizes (39 nm average grain size, 1.6 μ m thickness) was measured as > 280 W/m K with our measurement system. The effect of nanogranular microstructures on the thermal conductivity of metals has been studied with electrodeposited metal wires in other reports. For electrodeposited Ni, the thermal conductivity was shown to drop to 36.3 W/m K, which is 40% of the bulk

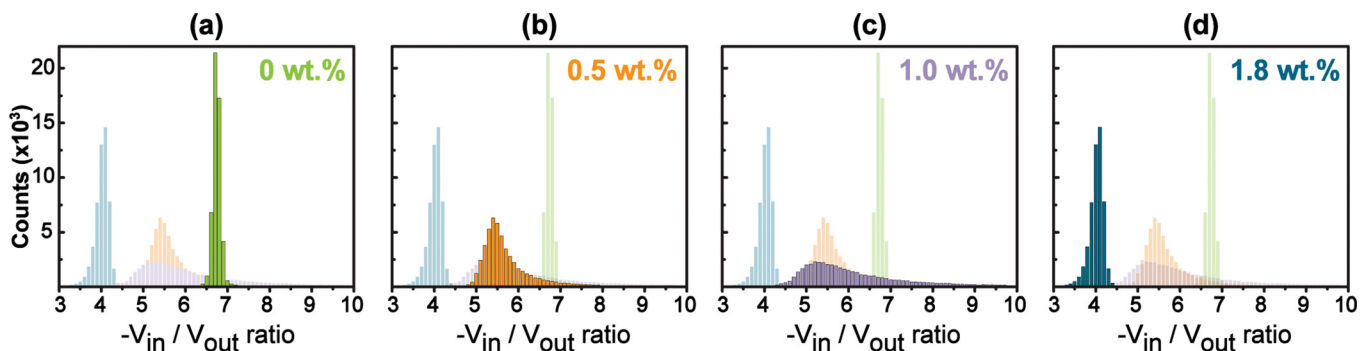


FIG. 3. (Color online) Histograms showing the distribution of the ratio values obtained from Cu-CNT composites with a (a) 0 wt. %; (b) 0.5 wt. %; (c) 1.0 wt. %; (d) 1.8 wt. % CNT content. All measurements were conducted at room temperature.

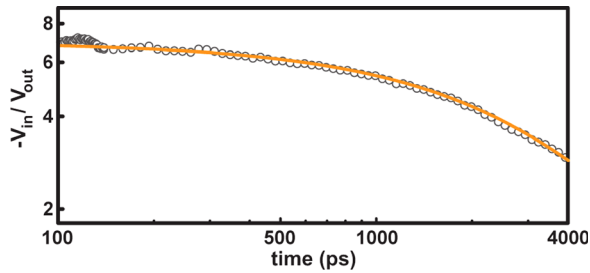


FIG. 4. (Color online) The cooling curve measured from the Cu-CNT composite with a 0.5 wt. % CNT content. (open circles) The measurement location was selected so that the $-V_{in}/V_{out}$ ratio at 940 ps matches the most frequent value determined from the distribution shown in Fig. 3(b). The solid line is from a thermal-model calculation.

value, as a result of reducing most of the grains to a size of ~ 10 nm.¹⁶ This size is comparable with the electron mean free path of Ni (6 nm). A similar effect was also observed with electrodeposited Ag wires.¹⁷

The depression in Λ caused by the addition of CNTs is understood in terms of increased electron scattering in the composite. To estimate the effect of electron scattering, we calculated the magnitude of the depression in Λ based on a model by Jongenburger¹⁸ assuming that vacancy scattering centers are present with an amount equivalent to the CNT volume (Fig. 5). Though exact agreement is not expected due to the discrepancy in the scattering origin, the estimated depression approximately matches the data, supporting the idea of electron scattering. This agreement is a significant indication that, in the Cu composite, the incorporated CNTs hardly contribute to heat conduction but rather impede the electronic transport, and thus the thermal transport. We also note that the sensitive dependency of Λ on the CNT content implies that any local variations of the CNT content can cause significant variations in the local thermal transport properties of the composite films. This conclusion supports the explanation that the CNT density variation in each sam-

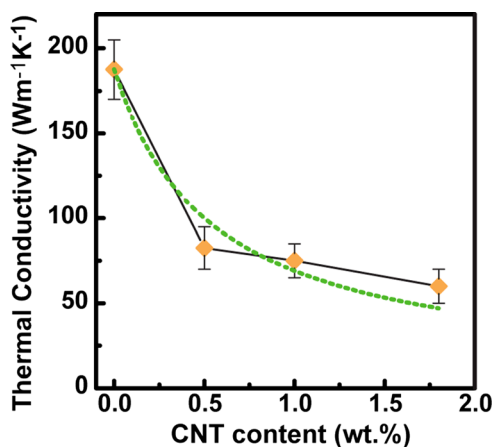


FIG. 5. (Color online) Thermal conductivity Λ values of the Cu-CNT composites (solid diamonds) obtained from model analysis of the representative cooling curves. Shown together is the calculated magnitude of the depression in Λ from volume-equivalent vacancy scattering centers (dotted line). For calculation, the value at 0 wt. % was taken from the measured data point, and the thermal conductivity was converted from electrical conductivity by means of the Wiedemann–Franz law.

ple is the main cause of the non-uniformity observed in the maps of thermal transport.

The identification of CNTs as scattering sources indicates that the thermal coupling through the interface between the Cu and CNTs is extremely poor. For the phonon-phonon coupling at the interface of Cu and CNTs, it has been reported that this route is even more resistive than CNT-polymer interfaces.¹⁹ Such phenomenon constitutes the understanding that the effective heat transport at CNT interfaces, where the bonding is weak, is through the low frequency phonon modes,^{20,21} while the number of phonon modes available at low frequencies is relatively small for metals. On the other hand, the direct coupling between electrons and phonons at the interface is generally considered as a non-significant process.²²

Another thermal coupling process to be considered is the electron-electron coupling through the interface between Cu and CNTs. Electron-electron coupling is known as the dominant coupling mechanism at metal-metal interfaces, being an order more conductive than typical phonon-phonon coupled interfaces.²³ Though CNTs are known as phonon-dominant heat conductors, the metallic character of MWCNTs calls upon for the consideration of this coupling process. However, our identification of the CNTs as thermal impediment sources indicates that the electron-electron thermal coupling between the Cu and the CNTs is also extremely poor in our samples. The electrical contact resistance between Cu and CNTs could possibly be related to the poor electron-electron coupling. In fact, a study observed that the electrical contact resistance between Cu and metallic CNTs is higher than well-wetting metals such as Ti, Cr, or Fe.²⁴ However, further examination of this aspect is beyond the scope of our present work.

This finding explains the difficulty of producing results conforming to the effective medium theory in metal-CNT composites. In addition, the highly resistive property of the interfaces between Cu and CNTs implies that greater dispersion of the CNTs can rather degrade the overall thermal transport capability more seriously.

V. SUMMARY

In summary, through a case study with Cu-CNT composite films, we demonstrated a procedure of determining the thermal conductivity of samples that are non-ideal for thin film thermal measurements. From the statistical distributions obtained by TDTR mapping, we were able to avoid complications from irregularities and non-uniformities. The determined thermal conductivity values of the Cu-CNT films revealed that the CNTs serve as a source impeding the heat transport in the host metal Cu.

ACKNOWLEDGMENTS

This work was supported by the Energy Efficiency & Resources program of KETEP granted by the Korean Ministry of Knowledge Economy (Grant No. 2008EID11P080000).

¹D. G. Cahill, W. K. Ford, K. E. Goodson, G. D. Mahan, A. Majumdar, H. J. Maris, R. Merlin, and S. R. Phillpot, *J. Appl. Phys.* **93**(2), 793 (2003).

- ²D. G. Cahill, *Rev. Sci. Instrum.* **75**(12), 5119 (2004).
- ³S. Huxtable, D. G. Cahill, V. Fauconnier, J. O. White, and J.-C. Zhao, *Nat Mater* **3**(5), 298 (2004).
- ⁴P. Kim, L. Shi, A. Majumdar, and P.L. McEuen, *Phys. Rev. Lett.* **87**(21), 215502 (2001).
- ⁵C. Yu, L. Shi, Z. Yao, D. Li, and A. Majumdar, *Nano Lett.* **5**(9), 1842 (2005).
- ⁶V. P. Veedu, A. Cao, X. Li, K. Ma, C. Soldano, S. Kar, P. M. Ajayan, and M. N. Ghasemi-Nejhad, *Nat. Mater* **5**(6), 457 (2006).
- ⁷F. H. Gojny, M. H. G. Wichmann, B. Fiedler, I. A. Kinloch, W. Bauhofer, A. H. Windle, and K. Schulte, *Polymer* **47**(6), 2036 (2006).
- ⁸M. J. Biercuk, M. C. Llaguno, M. Radosavljevic, J. K. Hyun, A. T. Johnson, and J. E. Fischer, *Appl. Phys. Lett.* **80**(15), 2767 (2002).
- ⁹H. Huang, C. H. Liu, Y. Wu, and S. Fan, *Adv. Mater.* **17**(13), 1652 (2005).
- ¹⁰R. Sivakumar, S. Guo, T. Nishimura, and Y. Kagawa, *Scr. Mater.* **56**(4), 265 (2007).
- ¹¹*CRC Handbook of Chemistry and Physics*, edited by D. R. Lide (CRC, Boca Raton, FL, 2005).
- ¹²K. Chu, Q. Wu, C. Jia, X. Liang, J. Nie, W. Tian, G. Gai, and H. Guo, *Compos. Sci. Technol.* **70**(2), 298 (2010).
- ¹³S. Cho, K. Kikuchi, T. Miyazaki, K. Takagi, A. Kawasaki, and T. Tsukada, *Scr. Mater.* **63**(4), 375 (2010).
- ¹⁴P. Nath and K. L. Chopra, *Thin Solid Films* **20**(1), 53 (1974).
- ¹⁵S. M. Rosnagel and T. S. Kuan, *J. Vac. Sci. Technol. B* **22**(1), 240 (2004).
- ¹⁶K. M. Razeeb and S. Roy, *J. Appl. Phys.* **103**(8), 084302 (2008).
- ¹⁷J. Xu, A. Munari, E. Dalton, A. Mathewson, and K. M. Razeeb, *J. Appl. Phys.* **106**(12), 124310 (2009).
- ¹⁸P. Jongenburger, *Phys. Rev.* **90**(4), 710 (1953).
- ¹⁹Q. Li, C. Liu, and S. Fan, *Nano Lett.* **9**(11), 3805 (2009).
- ²⁰S. T. Huxtable, D. G. Cahill, S. Shenogin, L. Xue, R. Ozisik, P. Barone, M. Usrey, M. S. Strano, G. Siddons, M. Shim, and P. Keblinski, *Nat. Mater.* **2**(11), 731 (2003).
- ²¹S. Shenogin, L. Xue, R. Ozisik, P. Keblinski, and D. G. Cahill, *J. Appl. Phys.* **95**(12), 8136 (2004).
- ²²H.-K. Lyee and D. G. Cahill, *Phys. Rev. B* **73**(14), 144301 (2006).
- ²³B. C. Gundrum, D. G. Cahill, and R. S. Averback, *Phys. Rev. B* **72**(24), 45426 (2005).
- ²⁴S. C. Lim, J. H. Jang, D. J. Bae, G. H. Han, S. Lee, I.-S. Yeo, and Y. H. Lee, *Appl. Phys. Lett.* **95**(26), 264103 (2009).